Influence of external mechanical loads on change of electrophysical characteristics of film sensor elements

Vladyslav Titarenko, PhD Yuliia Bondarenko
Cherkasy State Technological University, Cherkasy, Ukraine
julybo110976@gmail.com

***Abstract**: The materials of the article consider the influence of external mechanical loads of static and dynamic action (pressure force, mechanical impulse, vibration) on the change of electrophysical characteristics (electrical conductivity, specific capacitance) of film sensor elements. It is shown that an increase in the mechanical load on such an element with a simultaneous decrease in the interaction time with a constant contact area leads to an exponential increase in the power and sensitivity of the reaction pulse, provided that such mechanical load does not exceed the mechanical strength of the sensor element. At the same time, the increase in the mechanical load on the sensor element at constant time and contact area, almost does not change the sensitivity of the reaction pulse (the maximum increase in sensitivity does not exceed 1.8%). In this case, vibrational oscillations in the frequency range 30… 85 Hz at mechanical forces of the order of 20 … 150 mN create response pulses of the order of 12… 45 mV/μs, which are perceived as "false positives" of the sensor elements. A further increase in frequency and mechanical effort leads to the destruction of the base of the sensor element and the detachment of the sensor film from the base. Reducing the frequency and mechanical forces create reaction pulses up to 12 mV/μs, which does not exceed the allowable values of "white noise" (about 25… 35% of the minimum value of the reaction pulse).*

***Keywords:** FILM SENSOR ELEMENT, ELECTROPHYSICAL CHARACTERISTICS, MECHANICAL LOADS, VIBRATION, ELECTRICAL CONDUCTIVITY, SPECIFIC CAPACITANCE*

1. Introduction

Today in the electronics market there is a sharp increase in the number of products and their components containing sensory contact elements. This growth is primarily due to the continuous growth of products in the field of communications and entertainment, such as: mobile phones, tablets (and more recently stationary) PCs, game consoles, controls and settings for appliances, cars, multimedia devices and others [1]. This popularity and proliferation of devices with sensor elements leads to a gradual expansion of their areas of application, both in normal conditions (domestic use) and in extreme and/or emergency conditions of extreme pressures, temperatures, and especially power dynamic loads.

Thus, a number of leading domestic and foreign scientists deal with the development and research of sensory elements of electronic devices (E.Johnson, S.Hearst, B.Boy, W.Westerman, J.Elias, E.Wilson, J.Hahn, M.Krueger, T.Kuchmenko, A.Yurin, A.Dmitriev, V.Bochenkov, V.Zagorsky) [2-4] and large firms and research and production associations (HP, Bell Labs, IBM, BellSouth, Apple, Palm Inc., DSI Datotech, Samsung, Microsoft, ARIES, CitySensors) [5, 6].

However, the important issue of studying the electrophysical characteristics of film sensor elements of electronic devices in order to determine the impact of negative negative mechanical loads on them remains unresolved.

The aim of the work: to study the effect of external mechanical loads on the change of electrophysical characteristics of film sensor elements, which increases the accuracy, reliability and sensitivity of electronic devices, as well as to expand the range of performance of these devices in normal and extreme environmental conditions.

2. Basic requirements for sensor elements of electronic devices

The main type of materials used in the manufacture of capacitive layers are thin-film semiconductor materials [7]. Such film-forming semiconductors include systems of compounds connected by double or triple bonds (polyimides, polybenzimidazoles, polybenzoxazoles and others), as well as polymer complexes with charge transfer (halogenated polystyrene, poly-α-methylstyrene, etc.). The elements obtained from these materials have increased values of electrical and photoconductivity: 10^3-10^9 cm/m. In this case, the best coatings have high adhesion to the substrate and low values of water absorption and electrical conductivity (10^{16}-10^{17} Ohm·m). The most commonly used material in the application of functional sensor coatings is indium and tin oxide (ITO), the advantages of which are its transparency to the visible range of optical electromagnetic radiation and high electrical conductivity [8].

As a result of the analysis of literature sources [9, 10] for the rational mode of operation of sensor coatings of electronic devices there are certain requirements, which are the need to ensure guaranteed surface cleanliness prepared for the application of these coatings, as well as the proper choice of application.

The main problem in entering data from the projection-capacitive matrix is the strong dependence of the output signal on the type and design of the matrix, the high level of mechanical loads caused by external dynamic influences and the difficulty of adequate recognition and distinction of control signal from noise. In this case, the problem of data input from the projection-capacitive sensor matrix is the difficulty of recognizing the signal and converting it into coordinates, because the dependence of the amplitude and other characteristics of the output signal of a single segment of the matrix from distance to place is nonlinear. In addition, there are many side factors that complicate accurate coordinate recognition, such as high noise amplitude, mutual influence of matrix segments and the like. The solution to this problem is to establish the dependence of the output signals of the projection-capacitive sensor matrix on the position of the object of influence on the matrix in different methods of signal formation and measurement, as well as the development of an adequate mathematical model of analog signal conversion from the sensor matrix [11].

Therefore, the main factors that are necessary in compliance with the requirements for the quality of functional coatings are its reliable adhesion to the substrate (high adhesive and cohesive strengths that can be achieved by selecting technological modes of application of these coatings), as well as mechanical resistance and strength to external, both static and dynamic loads [9].

3. Features of determining the electrical characteristics of thin sensor coatings

Among the electrical characteristics of the ITO coating for film sensor elements should be noted the following [12-14]: electrical conductivity, resistivity, electrical capacity.

To maintain a high durability of maintaining the proper level of electrical characteristics of sensor coatings during their operation is to take into account their strength properties, which are known [15], depend on the coating material and its geometric characteristics.

Among the main geometric characteristics of functional coatings should be noted the following [16].

The geometric thickness of the coating is the shape of the controlled surface, which is characterized by a radius of curvature: $dr = 1 / S_0 \iint (Z_2 - Z_1)\, dS$, where S_0 – surface area of the substrate; dS is the differential element of this surface; Z_2 – surface of the substrate material; Z_1 – surface of the thin coating.

Effective coating thickness – the thickness of the coating that provides high conductivity of the surface material. Effective thickness is often associated with the measurement method. Effective in relation to this physical characteristic of the thickness is called the thickness of a homogeneous layer of a substance having the same properties as the actual coating.

In the general case, the radius of curvature *dr*, the effective weight thickness and the optical thickness coincide when the coating is uniform and homogeneous.

Internal and external forms of a covering. The external form is defined by the geometrical sizes of separate elements of a covering. The internal shape describes the crystal structure, type of lattice, orientation of the crystals, their size, defect, and so on.

Thus, to determine changes in the electrophysical characteristics of thin sensory coatings should take into account the following facts: the presence of donor oxygen vacancies, the presence of tin atoms, the use of colloidal metals, cationic substances, increased ionic current, increased substrate temperature, etc. [17, 18] geometric characteristics, such as geometric and effective coating thickness, internal and external forms of the coating [19], which have a significant impact on the durability of maintaining the proper level of electrical characteristics of these coatings.

4. Information and measuring stand for experimental testing of electrophysical characteristics of film sensor elements

A special information-measuring stand (IMS) was developed for experimental testing of electrical characteristics of film sensor coatings of electronic devices, where the objects of research were tested in a wide range of temperatures, humidity and dynamic mechanical loads.

The information-measuring stand (IMS) gives the chance to carry out research of electric characteristics in a wide range of values of external climatic (relative humidity and temperature) and mechanical (dynamic loading) factors. In this case, the measured values are in the range of values, which completely overlaps the range of their theoretical (calculated) values.

The general view of IMS is shown in Fig.1, and its measuring characteristics – in table.1.

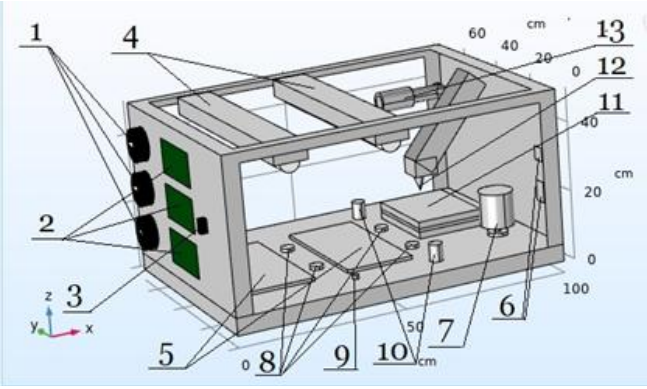

Fig.1. *Appearance of the information and measuring stand: 1 - handles of adjustment of parameters of factors of influence; 2 - indicators of the stand operation status; 3 - on-off button; 4 - quartz heaters; 5 - holders for establishing the object of study; 6 - connectors for connection to a PC and to the mains; 7 - vibrating motor; 8 - ultrasonic moisture spray; 9 - microwave resonator; 10 - humidity regulator; 11 - subject table; 12 - measuring probe of electrical and mechanical characteristics from the surface of the touch screen; 13 - piezodrive of the probe (pos.12)*

The main technical characteristics of the stand are as follows: operating temperature range: -30…+80 ºC (±0.5-1%); relative humidity: 0-85% (±2-3%); vibration oscillations: up to 0.45 mm/s (±3-5%).

Table 1. *Measuring characteristics of the information-measuring stand*

Measuring characteristics	Range of values	Relative measurement error, %
Specific electrical resistance, $\times 10^{-6}$, ohm·m	5 – 500	± (1,5 – 2,5)
Electric capacity, $\times 10^{-12}$, F	$10 – 1{,}2 \cdot 10^{6}$	± (2 – 3,5)
Surface conductivity, $\times 10^{3}$, ohm^{-1}	0,2 – 200	± (3 – 4,5)

The main element of such a stand is the control and monitoring system developed by the author, which includes two units that simulate climatic and power conditions and two measuring circuits - electrical characteristics and mechanical loads.

The principle of IMS is as follows. The object of study, was installed in special holders (pos.5), and was exposed to simultaneous thermal, vibration and humidity. The IMS was connected to a PC (pos.6), and the sensitivity and fault tolerance of the objects of the study were tested in a wide range of parameters of the above external factors in real time. According to the results of the test experiment, the researcher determined the minimum allowable probability of the operating state of the sensor sample. At the next stage, the probability of working condition of each sample was compared with their minimum allowable value. If this condition is not met, in order to increase the probability of working condition of the sensors, the researcher is given a recommendation to replace one of the established samples, the probability of failure of which has reached a minimum at the moment.

Thus, the developed test equipment (IMS) for studying the electrophysical characteristics of the film sensor elements of electronic devices, allows to determine with high accuracy the characteristics of these coatings, such as: conductivity, resistivity and capacitance. In this case, the error in determining the electrical conductivity did not exceed 4.5%, resistivity - 2.5%, capacitance - 3.5%. This allows us to draw conclusions about the rapid and qualitative determination of such electrophysical characteristics of film sensor elements in a wide range of values of mechanical (force dynamic) loads, than to adjust the operating range of values of these factors when using such sensor coatings in normal and extreme operating conditions.

5. Algorithm for determining the effect of mechanical loads on the change of electrophysical characteristics of film sensor elements

Determination of the electrical characteristics of the film sensors from the action of external mechanical loads was performed using the contact mode of interaction of the measuring probe IMS with the surface of the test sample. The adjustment of the mechanical dynamic load was performed using an adjustable electric drive IMS.

The sequence of determining the influence of external mechanical dynamic loads on the change of electrical characteristics of thin coatings.

I. Investigation of the influence of friction coefficient and adhesive strength of coatings.

1. The study of the influence of the coefficient of friction and the adhesive strength of coatings is carried out by measuring scratching (sclerometry) with a measuring probe.

1.1 The sample is mounted on a slide, which moves together with the micrometer platform for positioning or scratching in three coordinate planes, which occurs under the action of precision electric motors with built-in micrometer displacement sensors

2. In the "nanoindentation" mode, the dependence of the load on the depth of penetration of the probe is built.

2.1 There is a penetration of the measuring probe into the coating. In this case, this depth of penetration should not exceed 10-12% of the coating thickness.

2.2 Several superimposed hysteresis curves "load - immersion depth" are obtained.

2.3 The value of microhardness, modulus of elasticity and elastic recovery is calculated using specialized software (for example, "NanoTest 600").

2.4 To calculate the above module, the Oliver-Farr model is used, according to which a part of the dependence "load - depth of penetration" during unloading is described. The method consists in approximating the initial section of the discharge curve of the power function $P_{max} = B(h - h_f)^m$, where P_{max} is the maximum load, h is the depth of penetration of the indenter,

2.5 The slope of the initial stage of the unloading curve determines the stiffness of the material:

$$S = \left(\frac{dP}{dh}\right)_{h=h_{max}} = mB\left(h_{max} - h_f\right)^{m-1}. \quad (1)$$

2.6 Calculate the penetration depth of the indenter h_c:

$$h_c = h_{max} - \varepsilon\frac{P_{max}}{S}, \quad (2)$$

where h_{max} is the maximum depth of penetration of the indenter; the coefficient $\varepsilon = 0.75$:

$$\boldsymbol{H = \frac{P_{max}}{A}}, \quad \boldsymbol{E_{eff} = \frac{1}{\beta}\frac{\sqrt{\pi}}{2}\frac{S}{\sqrt{A}}}; \quad \boldsymbol{\frac{1}{E_{eff}} = \frac{1-\nu^2}{E} + \frac{1-\nu_i^2}{E_i}}, \quad (3)$$

where ν is the Poisson's ratio of the coating, the coefficient β = 1,034 - for the measuring probe; A - the projection area of the imprint is determined from the depth of the maximum penetration of the indenter h_{max}. For a diamond indenter, the Poisson's ratio ν_i = 0.07, and the elastic model E_i = 1141 GPa. The amount of elastic recovery of coatings is determined by the formula:

$$\boldsymbol{W_e = \frac{(h_{max} - h_f)}{h_{max}}}. \quad (4)$$

2.7 By pressing the indenter in the sample with a constantly increasing load is measured values: internal stress, acoustic emission intensity, friction force, friction coefficient and depth of scratching, Fig.2.

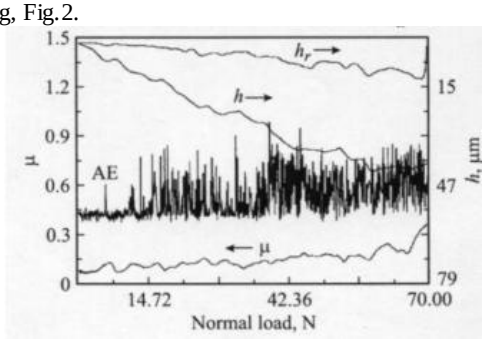

a.

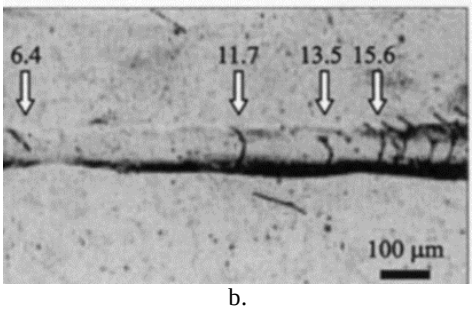

b.

Fig. 2. *The results of adhesion tests of the "coating-substrate" system: a – dependences of acoustic emission (AE), coefficients of friction μ, depth of penetration of indenter h and final depth of scratching h_r; b – structure of the coating in the fracture zone*

The procedure for testing in this method is as follows:

1) Before the start of the tests, the system (pendulum, load, etc.) is calibrated using a calibrated sample of fused quartz.

2) The test specimen is mounted on a platform stage.

3) Before the start of measurements, the sample table with the sample is brought into contact with the probe at a safe speed (3.8 μm/s), and then removed to a distance of 25 μm.

4) The measurement process is performed automatically according to a pre-prepared program (includes 10 cycles "load-unload" with a maximum value of load 200 mN and a rate of increase and decrease of load 10 mN/s with an indentation between individual contacts 20 μm along the Z axis).

5) After the measurement is completed, a software analysis of the obtained curves is performed, which allows to obtain the values of hardness, elasticity and elastic recovery of the coating.

6) The study of mechanical characteristics in depth is carried out for a batch of samples before and after each tribological examination.

7) Scratching occurs automatically according to a pre-prepared program: the load is continuously increasing from 0.5 to 200 mN at a speed of 5 mN/s; the length of the scratch is 100 μm.

8) Upon completion of scratching, a visual examination of the sample is performed - using an optical microscope and changing one of the parameters (acoustic emission, friction force, coefficient of friction, depth of penetration of the probe or final depth of scratch), fixes the moment of adhesive or cohesive destruction (critical) load, which leads to its destruction.

9) In the mode of repeated remote scanning of the surface, get a map of the distribution of residual electric charge on the surface of the study area.

10) With the help of specialized software, the values of capacitance, electrical conductivity and surface resistance are calculated.

Thus, a method for studying the effect of external dynamic mechanical loads on the electrophysical characteristics of sensor coatings obtained using the developed IMS, the use of which allows to establish the effect of dynamic mechanical loads on the electrophysical characteristics (conductivity, resistivity and capacitance of the sensory coating) of electronic devices.

6. Analytical modeling of electrical processes occurring in the coatings of sensor elements from the action of mechanical loads

Under conditions of thermodynamic equilibrium, the calculation of the electrical characteristics of the p-n junction, namely: the built-in electric field and the distribution of charge carriers, is based on the Poisson equation:

$$\frac{d^2\phi(x)}{dx^2} = \frac{4\pi e}{k_0}[n(x) - N_d - p(x) + N_a(x)], \quad (5)$$

where, $\phi(x)$ is the electrostatic potential, e is the elementary charge, k_0 is the static dielectric constant.

The concentration of donors N_d=const corresponds to a homogeneous n-doping of the original sample, and the concentration of acceptors $N_a(x)$ is determined by the parameters of ion doping.

It is believed that all donor and acceptor levels are ionized. If the degeneracy of the charge carriers of the concentration of electrons $n(x)$ and holes $p(x)$ is arbitrary, then they are self-consistently associated with the electrostatic potential, according to the following relations:

$$n(x) = N_c F_{1/2}\left[\frac{\varepsilon_F \cdot g_a + e\cdot\phi(x)}{k_B T}\right]; \quad (6)$$

$$p(x) = N_v F_{1/2}\left[\frac{-\varepsilon_F \cdot g_a - \varepsilon_g - e\cdot\phi(x)}{k_B T}\right]. \quad (6')$$

where $N_{c,v} = \frac{\sqrt{2}\,(m_{c,V}\cdot k_B T)^{3/2}}{\pi^2 h^3}$ is the effective density of states in the conduction band (c) and the valence band (v), m_c is the effective mass of the electron, m_v is the effective mass of the holes, h is the Dirac constant and T, g_a is the temperature and absolute humidity of the environment, and the functions $F_{1/2}$ are Fermi-Dirac integrals.

Equations (6)-(6') are obtained under the assumption of the parabolic law of carrier dispersion, where ε_g is the band gap.

Equations (5)-(6') form a nonlinear differential equation of the second order, which for an arbitrary thin layer $N_a(x)$, is possible to solve by the finite element method, within the Cauchy problem with boundary conditions.

$$\varphi(-L^{'}n) = 0, \varphi(-L^{'}p) = \Phi_b, \quad (7)$$

In the depth of the quasi-neutral n-region, a zero potential equal to a certain value of Φ_b (height of the built-in electrostatic potential) is selected. The constants Φ_b and ε_F are unknown, but must satisfy the conditions of charge neutrality within the $n(x = -L_n)$ and $p(x = L_p)$ domains.

It is known [20] that the region of the spatial charge has a size of about 1.5-2 μm. In this case, the potential distribution shows a bimodal behavior that is absent for the standard profile of the sensory *n-p* junction with sharp doping. The resulting size of the space charge region is proportional to the characteristic length of the absorption of infrared radiation, which makes it possible to detect infrared radiation.

In regions deeper than 3 μm, a quasi-neutral n-region is realized, where the concentrations of the main carriers (electrons) are approximately N_d, and the concentration of non-basic carriers (holes) is orders of magnitude lower than in the p-region. It is important to note that in the depth of the *p*-region the electron gas of the holes remains degenerate (the Fermi level lies in the valence band).

To describe the transfer of carriers in the electric *p-n* junction, a drift diffusion model is used, which characterizes the following system of equations:

$$\frac{d^2\varphi(x)}{dx^2} = \frac{4\pi e}{k_0}[n(x) - N_d - p(x) + N_a(x)]; \; E(x) = -\frac{d\varphi}{dx} \quad (8)$$

$$j_n(x) = e\mu_n n(x)E(x) + eD_n\frac{dn(x)}{dx} \quad (9)$$

$$j_p(x) = e\mu_p p(x)E(x) + eD_p\frac{dp(x)}{dx} \quad (10)$$

$$\frac{1}{e}\frac{dj_n(x)}{dx} = -\left(G^+(x) - G^-(x)\right); \frac{1}{e}\frac{dj_p(x)}{dx} = \left(G^+(x) - G^-(x)\right); \quad (11)$$

$$j \equiv j_n(x) + j_p(x) = const \quad (12)$$

where j_n and j_p are the partial currents of electrons and holes, respectively (total current through the p-n junction is a constant), and $\mu_{n,p}$ and $D_{n,p}$ are their mobility and diffusion coefficients.

In the case of an nonequilibrium state, the concentrations of electrons and holes are determined by the local quasi-Fermi levels $\varepsilon_n(x)$ and $\varepsilon_p(x)$, which are functions of coordinates:

$$n(x) = N_c F_{\frac{1}{2}}\left[\frac{\varepsilon_n(x)\cdot g_a^{2/3} + e\cdot\varphi(x)}{k_B T}\right];$$

$$p(x) = N_v F_{\frac{1}{2}}\left[\frac{-\varepsilon_p(x)\cdot g_a^{1/3} - \varepsilon_g - e\varphi(x)}{k_B T}\right] \quad (13)$$

In the equation of continuity 12, the values of $G^{\pm}(x)$ correspond to the generation and recombination of electron-hole pairs. The model of direct generation and recombination was used, within which $G^{\pm}(x) - G^{-}(x) = -\gamma[n(x)p(x) - n_0p_0]$ where γ is the volume recombination coefficient. Equation (13) is supplemented by boundary conditions that assume a model of ohmic contacts:

$$\varphi(-L^{'}_n) = 0; \; \varphi\left(-L^{'}_p\right) = \Phi_b + \frac{U_D}{e};$$

$$\varepsilon_n(-L'_n) = \varepsilon_p(-L'_n) = \varepsilon_F; \; \varepsilon_n\left(L'_p\right) = \varepsilon_p\left(L'_p\right) = \varepsilon_F - U_D, \quad (14)$$

where the equilibrium parameters Φ_b and ε_F can be obtained from the previous section, and U_D is the applied voltage.

When calculating the volt-ampere characteristics, it is taken into account that the recombination times of holes in the n-region and electrons in the *p*-region depend on the corresponding concentrations. Therefore, the recombination coefficients in the *n*- and *p*-domains can be expressed as $\gamma_n(x) = \left[\tau_p(\varepsilon_F\cdot g_a + \varepsilon_g + e\cdot\varphi(x))n(x) - 1\right.$ and $\gamma px = \tau n(\varepsilon F\cdot ga + \varepsilon g + e\cdot\varphi(x))p(x) - 1$, respectively.

As a result, $\gamma(x) = \gamma_n(x)$ for $x < x_{ch}$ and $\gamma(x) < \gamma_p(x)$ for $x > x_{ch}$ is characterized by a coordinate at which $\gamma_p(x_{ch}) = \gamma_n(x_{ch})$.

It is seen that $\gamma(x)$ in the *n*- and *p*-domains takes the values $\gamma \approx 10^{-9}$ and $\gamma \approx 3\cdot10^{-10}$ cm^3/s, respectively and significantly increases its values to 10^{-5} cm^3/s in the region of space charge. As calculations have shown, the quasineutral region can be considered as part of the contact resistance R_c.

Thus, the analytical dependences of electrical processes occurring in the functional coatings of the sensor elements of electronic devices are obtained. However, some differences in analytical calculations can be explained by several factors that do not take into account the classical theory. In particular, such film sensor elements may have additional current transfer mechanisms that may be associated with barrier tunneling effects, electrical breakdown effects caused by strong internal fields, and so on. Classical theory also does not take into account leakage currents through surface states in the real two-dimensional configuration of the sensor element.

7. Development of a computer mathematical model of the electrophysical characteristics of sensory elements

To study the electrical properties of electrically conductive thin ITO film, the finite element method is used. In this case, numerical simulation of the electrical properties of a 3D model of a thin touch film is performed using Comsol Multiphysics.

To implement the finite element method, Maxwell's equation is used in terms of electric potential:

$$-\nabla\times\left(\left(\sigma + \varepsilon_r\varepsilon_0\frac{\partial}{\partial t}\right)\nabla V\right) = 0 \quad (15)$$

where, σ is the electrical conductivity of the material; ε_r – relative dielectric constant; ε_0 – vacuum dielectric constant (8.854×10^{-12} F/m);

After that, the problem was reduced to solving the electric potential in each region of finite elements.

Other electrical characteristics, such as resistivity (*Z*) and electrical capacitance (*C*), can be determined by the following formulas, respectively:

$$Z = \frac{1}{\gamma} = Z^{'} + jZ^{''} \quad (16)$$

$$C = C^{'} + jC^{''} = \frac{\gamma^{''}}{\omega} + j\frac{\gamma^{'}}{\omega} \quad (17)$$

In this case, the modeling of the ITO film is considered as a homogeneous layer without defects and porosity.

The procedure for setting up simulation in Comsol Multiphysics is as follows:

- the 3D model and the interface of electric currents AC/DC are selected in the Comsol modeling menu;
- geometric modeling of a thin film is carried out;
- an appropriate modeling grid is created;
- the electrical parameters of the test material are determined;
- the model is calculated by the correct expression in the study of the frequency domain.

There is a final transformation of the calculated data into other electrical properties.

The results of numerical studies. In the proposed computer model, the upper plane of the object is the electrode of the sensor element. ITO film (20 mm × 20 mm × 10 μm) is applied on top of the substrate (quartz glass: 20 mm × 20 mm × 0.2 mm), which is surrounded by air (25 mm × 25 mm × 1 mm). This model (Fig. 3) best mimics the real object of study.

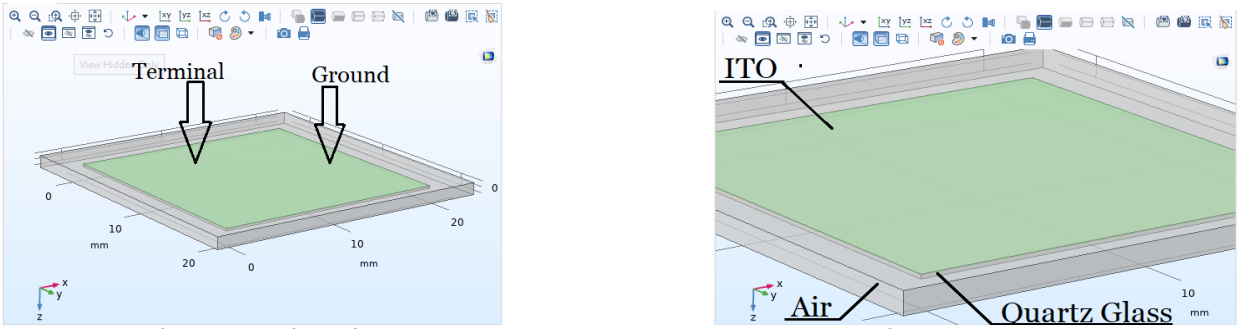

Geometric parameters of the 3D model for configuring measurements in the plane *Model of the object under study*

Fig. 3. *Image of the simulated object (film sensor element)*

The low electrical potential of the surface of the ITO film is installed on the conductive substrate, except for the area in the area of the electrodes. The largest dispersion of the electric potential for the insulating substrate is demonstrated near the region of the electrodes. It should also be noted that when measuring the ITO film on the conductive substrate, only the ITO region and the single crystal substrate have a significant effect on the current direction.

Simulated impedance and capacitance values from 0.1 Hz to 10 MHz for the same 10 µm ITO film also demonstrated that the measurement configurations can cause very large differences in the electrical characteristics of this film, Fig. 4.

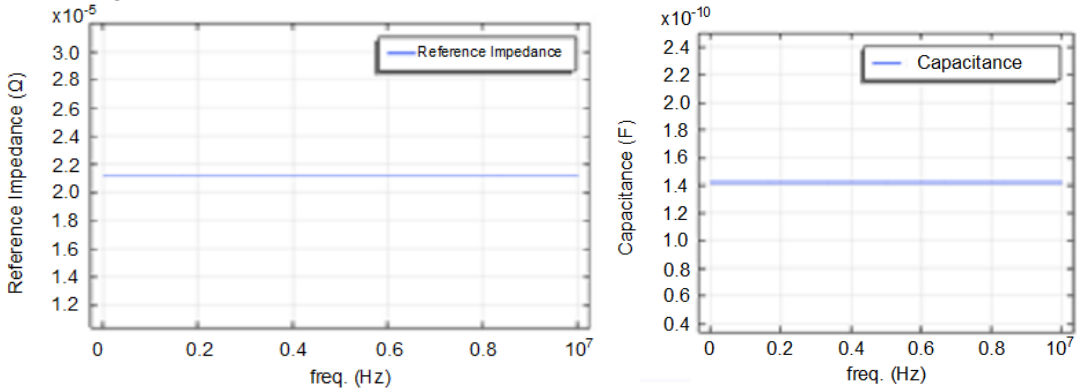

Fig. 4. *The results of the calculation of the impedance (left) and capacitance (right) for the ITO sensor film in the frequency range 10^{-1} – 10^{6} Hz*

For example, the impedance values of 1 Hz for ITO film (20 mm × 20 mm × 10 µm) can vary from $5{,}247 \cdot 10^{-5}$ Ohms for parallel plate configuration to 100.8 Ohms for in-plane measurements on insulating material. The actual capacitance at an operating frequency of 1 Hz can vary from $5.712 \cdot 10^{-4}$ µF (plate thickness) to about 10^{-3} pF (along the plane). These values can also be used to verify the accuracy of the model. According to the equations of resistance and capacitance for parallel plates 4 and 5 were:

$$R = \frac{\rho L}{A} = \frac{t}{\sigma a^2} = \frac{10 \cdot 10^{-6}}{1180 \cdot (20 \cdot 10^{-3})^2} = 2{,}118 \times 10^{-5} \text{ ohm}$$

$$C = \frac{\varepsilon_r \varepsilon_0 A}{d} = \frac{\varepsilon_r \varepsilon_0 a^2}{t} = \frac{4 \cdot 8.854 \cdot 10^{-12} \cdot (20 \cdot 10^{-3})^2}{10 \cdot 10^{-6}} = 1{,}416 \times 10^{-10} \text{ F}$$

Thus, the simulation results show that the configuration of the parallel plate and the configuration in the plane with the conductive substrate show a relatively low value of impedance. Given the existence of conductor resistance and contact, it is very difficult to obtain a real electrical reaction of the ITO film from the results of real experimental measurements. In addition, at very low resistance, the imaginary impedance of the circuit will be dominated by the inductance of the circuit, which can not show the correct capacitive behavior. Thus, the measurement in the plane with the insulating substrate, which has a relatively large value of impedance - minimizes the impact of the environment.

Influence of material and air environment. As insulating materials, the quartz glass substrate and the air environment have high impedance values in real conditions. Simplified 3D models were used to model the impedance and capacitance of a combination of ITO film with a quartz substrate, a combination of ITO film with air, a combination of ITO with both a substrate and air. Thus, it became possible to divide and compare the electrical characteristics of each material. Thus, the quartz substrate and the air layer are insulated, and their impedances decrease with increasing frequency. The ITO film with a thickness of 10 µm and its three combinations with the surrounding materials had the same impedance of 10^4 Ohms. Imaginary impedances have always been close to zero compared to real impedances. Thus, the value of the calculated impedance is close to the actual value of the real impedance. Thus, it was concluded that the material and the air have little effect on the impedance of the ITO film.

However, the values of the received capacities showed different tendencies. Thus, clean substrate ($3.15 \cdot 10^{-14}$ F) and clean air ($7.51 \cdot 10^{-15}$ F) have a much larger capacity than pure ITO film ($3 \cdot 10^{-18}$ F, within the estimate of 10^{-19} F to 10^{-17} F). As a result, the capacities of the combined systems are close to the substrate capacity and the air capacity, more than two orders of magnitude higher than the capacity of the ITO film, even showing a transition in the middle frequency range (10 to 10^4 Hz).

8. Comparison of the results of analytical and mathematical modeling of the electrophysical characteristics of sensory elements from the action of mechanical loads

The comparison of the results of analytical and mathematical modeling is presented in Fig. 5, shows the difference between simulation under thermodynamic equilibrium and simulation using the finite element method.

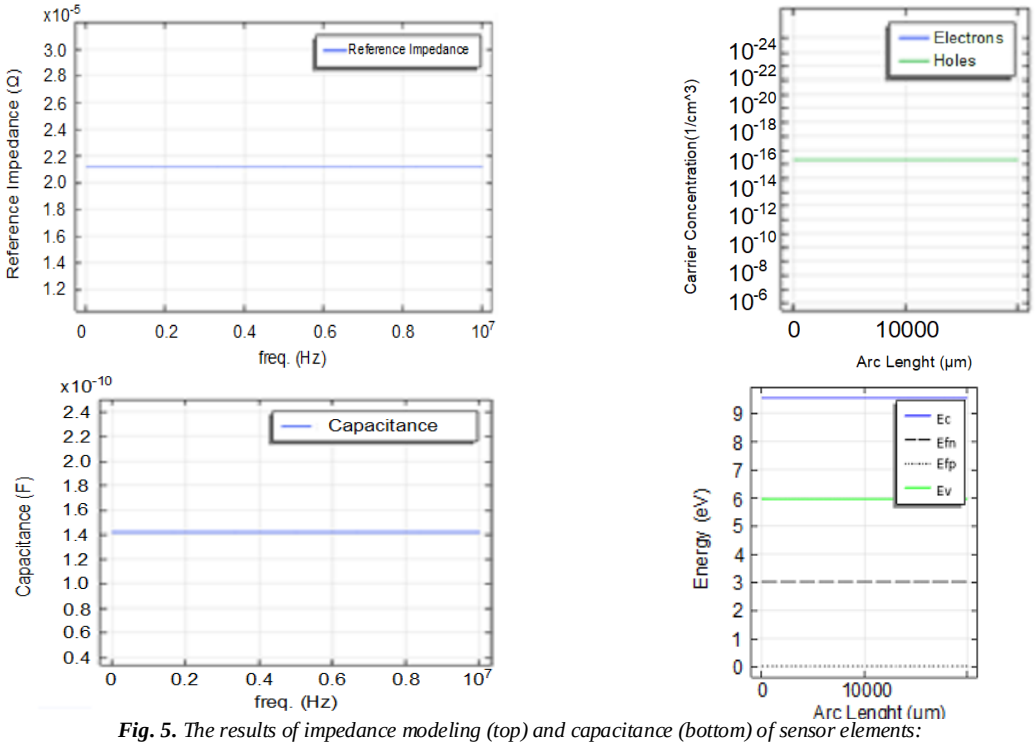

Fig. 5. *The results of impedance modeling (top) and capacitance (bottom) of sensor elements: on the left - the results of numerical modeling, on the right - the results of analytical modeling: Ec - conduction band energy level; Efn - electron quazi-fermi energy level; Efp - hole quazi-fermi energy level; Ev - Valence band energy level*

The simulation was performed using COMSOL software. A two-dimensional semiconductor model was used for analytical modeling, namely, the energy zones for the semiconductor and the frequency properties of the p-n junction were studied.

A three-dimensional model of a thin-film semiconductor was used for numerical simulations, namely: resistivity, electrical conductivity and electrical capacitance were studied.

The results obtained as a result of modeling the electrophysical characteristics of the sensor device take into account the results of stationary and frequency studies.

The main task of the study was to measure the characteristics to identify the performance of the sensor device in extreme conditions.

Thus, as a result of mathematical modeling of electrical processes occurring in the film sensor elements of electronic devices from the action of mechanical loads, the study of electrophysical processes occurring under normal and extreme conditions is performed.

Analytical and numerical modeling of the investigated surface of the sensor device was performed.

In the case of analytical modeling, the electrical characteristics of the p-n junction of the investigated semiconductor were calculated, namely the built-in electric field and charge carrier distribution from changes in internal voltages and, accordingly, the carrier concentration in the semiconductor.

In the case of numerical simulation, the COMSOL software was used, which allows to do research by the finite element method, which uses the Maxwell equation, in terms of electric potential. Measurement of electrical conductivity, capacitance and resistivity was performed in the frequency range 10^{-1}–10^{7} Hz, in the conditions of finding the sensor coating on the insulating substrate in the ambient air.

5. Conclusion

As a result of research the following is established:

- increasing the mechanical load on the thin-film sensor element with a simultaneous decrease in the interaction time with a constant contact area leads to an exponential increase in power and sensitivity of the reaction pulse, provided that such mechanical load does not exceed the mechanical strength of the sensor element material;
- increase in mechanical load on the sensor element for a constant time and contact area, almost does not change the sensitivity of the reaction pulse (maximum increase in sensitivity does not exceed 1.8%);
- vibrational oscillations in the frequency range of 30-85 Hz at mechanical forces of the order of 20-150 mN create response pulses of the order of 12-45 mV/μs, which are perceived as "false operation" of sensor elements;
- increasing the frequency and mechanical forces above the specified range leads to the destruction of the base of the sensor element and the detachment of the sensor film from the base;
- reduction of frequency and mechanical forces below the specified range create reaction pulses up to 12 mV/μs, which does not exceed the permissible values of "white noise" (about 25-35% of the minimum value of the reaction pulse).

6. Literature

1. Trends in science and technology 2020-2040. As evidenced by a NATO study. Part 1 [Online]. Available: http://opk.com.ua/%D1%82%D1%80% D0% B5% D0% BD% D0% B4% D0% B8-% D0% B2-% D0% BD% D0% B0 % D1% 83% D1% 86% D1% 96-% D1% 82% D0% B0-% D1% 82% D0% B5% D1% 85% D0% BD% D0% BE% D0% BB% D0% BE % D0% B3% D1% 96% D1% 8F% D1% 852020-2040-% D0% BF% D1% 80% D0% BE-% D1% 89% D0% BE /. Accessed on: October 7, 2018
2. M.Kaltenbacher, *Numerical Simulation of Mechatronic Sensors and Actuators Finite Elements for Computational Multiphysics*, (Springer Berlin Heidelberg, Berlin, Germany, 2015).
3. Jerome P. Lynch, *Sensors and Smart Structures Technologies for Civil, Mechanical, and Aerospace Systems*, (2015).
4. Kara J. Peters, *Smart Sensor Phenomena, Technology, Networks, and Systems Integration*, (2015).
5. Global Wireless Sensor Network Research Report 2019 to 2026 [Online]. Available: https://www.itintelligencemarkets.com/request_sample.php?id=85. Accessed on November 7, 2018.
6. Cellphone Fingerprint Recognition Sensor Market Witness High Growth And Manufacturing Analysis By 2027 | Apple,

Synaptics, Fingerprints [Online]. Available: https://neighborwebsj.com/uncategorized/943676/cellphone-fingerprint-recognition-sensor-market-witness-high-growth-and-manufacturing-analysis-by-2027apple-synaptics-fingerprints/ Accessed on January 6, 2021 .
7. D.Dehtyarenko, V.Mikulko, V.Ejov, in: *Actual problems of energy*, (2016), pp. 446-450. *(in Russian)*
8. L.Amosova, M.Isaev, J. Tech. Phys., 10(84), 127 (2014). *(in Russian)*
9. K.L.Mittal, Electrocomp. Sci. Tech., 3, 21-24 (2007).
10. Polymer-tech. Cohesive strength. [Online]. Available: http://polymer-tech.ru/ref/kogezionna9_pro2nost5.html#allref Accessed on December 20, 2018.
11. The problem of data entry from the projection-capacitive sensor matrix [Online]. Available: http://ptsj.ru/articles/45/45.pdf Accessed on December 15, 2019.
12. PERSISTENCE Merket Search - Thin Film Capacitor Market [Online] Available: https://www.persistencemarketresearch.com/market-research/thin-film-capacitor-market.asp Accessed on June 18, 2019.
13. Techinstro - ITO Coated Glass [Online]. Available: https://www.techinstro.com/ito-coated-glass/ Accessed on July 15, 2019.
14. Hart Materials - The use of nickel based particles in the electronics industry [Online]. Available: https://www.hartmaterials.com/images/documents/the%20use%20of%20nickel%20based%20particles%20in%20the%20electronics%20industry.pdf Accessed on Sptember 5, 2019.
15. Encyclopedia of Mechanical Engineering XXL - Methods for determining the adhesive strength of films [Online]. Available: https://mash-xxl.info/info/585429/ Accessed on December 20, 2019.
16. NPP Electrochemistry Galvanic coatings and metalworking, Non-destructive methods of thickness control [Online]. Available: https://zctc.ru/sections/metodi_kontrolya_tolshini_pokritiya Accessed on December 25, 2018.
17. Chia-Ching Wu, Chien-Chen Diao, in: *MATEC Web of Conferences*, (Iss.185, 2018), pp. 1-6.
18. Shiuh-Chuan Her, Chun-Fu Chang, J. Appl. Biomater., 15(2), 170-175 (2017).
19. ScienceDirect - Film Thickness [Online]. Available: https://www.sciencedirect.com/topics/materials-science/film-thickness Accessed on February 17, 2021.
20. The area of the spatial charge of the p-n junction [Online]. Available: https://studfile.net/preview/1906091/page:4/ Accessed on April, 15.